APPLIANCE OF SCALING METHODOLOGIES FOR DESIGNING COUNTERPART EXPERIMENTS DOMINATED BY NATURAL CIRCULATION PHENOMENA

M. Lorduy-Alós, S. Gallardo and G. Verdú

Instituto Universitario de Seguridad Industrial, Radiofísica y Medioambiental

Universitat Politècnica de València, València, Spain.

Abstract

The utility of the Integral Test Facilities (ITF) for the study of thermohydraulic phenomena that can occur in nuclear power plants has been demonstrated. However, direct extrapolation of data between different scales is challenged due to the uncertainty and distortion that implies the application of scaling laws. In this sense, the analyses of counterpart experiments help to clarify the capabilities and limitations of scaling methodologies.

This work focuses on the design and study of a counterpart experiment in the LSTF facility based on the ATLAS A1.1 test. The transient at issue reproduces a SBO-type scenario with the asymmetric and delayed supply of auxiliary feedwater. The scenario in ATLAS and LSTF facilities is simulated with the TRACE5 thermal-hydraulic code and the results are compared. Then, a global system scaling analysis is performed and the calculation of dimensionless groups reveals, through an analytical approach, the relevance of the transfer processes (mass, enthalpy and so on) in the evolution of the transient and the scaling distortion between both facilities.

This study assesses a great similarity in the evolution of the main thermal-hydraulic phenomena throughout the experiment, despite a significant discrepancy is evidenced in the chronology. Likewise, the results support the novel procedure to design the counterpart test.

Keywords: Scaling; counterpart; natural circulation; ATLAS; LSTF

1 INTRODUCTION

In the past few decades, plenty of Integral Test Facilities (ITF) have been built worldwide aimed at solving safety concerns in the nuclear field [1]. The experiments carried out in ITFs afford valuable databases helpful in identifying and understanding the thermal-hydraulic phenomena that may occur in the Nuclear Power Plants (NPP). These tests enable analyzing scenarios that cannot be reproduced in an NPP since usually, only data for mild operational transients are accessible. Furthermore, the relevant nuclear safety regulations require the validation of the thermal-hydraulic code against experimental data from nuclear power plants and test facilities [2]. In this process, the extensive databases generated in ITFs are worthwhile for code development, update and verification.

Some of the main advantages of the test facilities are their reduced-scale design compared to a reference reactor, which implies the cost reduction for both construction and operation, the availability of many measurements of different parameters, and the possibility for recreating severe accidental scenarios by avoiding the risk entailed at a real plant. However, the use of these data to predict the behavior of an NPP is challenged due to the uncertainty and distortion that implies the application of scaling laws, which are not always fully trusted [3]. This has motivated the performance of counterpart

tests (CT) between facilities to demonstrate that similar phenomena occur at different scales. the counterpart tests require the same prototype NPP for the ITF involved in the CT and preservation of the following initial and boundary conditions [4] and, if these requirements are met, the distortions due to heat losses, bypass flows, downcomer configuration or heater rod elements are reduced.

- Thermodynamic state (pressure, temperature and flow condition).
- Scaled mass flow rate
- Power to volume ratio
- Heat and mass sources and sinks (e.g. location and size of break).
- Action-based on actual signals (e.g. safety injections systems operation).

Under this premise, no experiment performed in any ITF can be considered strictly the CT of any other test in a different ITF. However, the experiments whose initial and boundary conditions have been properly scaled and adjusted according to a scaling method are recognized as a CT and are feasible to be part of counterpart activities. Hence, these experiments are not considered only similar, and this term is relegated to another type of test. Specifically, similar tests (ST) usually refer to those CTs whose initial or boundary conditions are not fully aligned with the above criteria. One of the most representative examples is the variety of experiments on natural circulation (NC) behavior performed in all major ITFs aimed at commissioning the facility and characterizing the phenomenon. The results of these tests have served to build an NC flow map (core inlet flow rate/core power Vs primary system inventory/volume) and an envelope to predict NC situations in a typical PWR [5].

Most counterpart tests have been focused on the study of experiments that meet these characteristics. One of the most significant campaigns on a SBLOCA counterpart scenario included four facilities, covering a broad range of volume scaling ratios: LOBI (1:712), SPES (1:427), BETHSY (1:100) and LSTF (1:48) [6]. The experimental results together with all the analytical work confirmed the capability of the facilities to reproduce a typical PWR behavior considering suitable initial and boundary conditions [7] [8] [9].

Based on the premise that it is the phenomena, not the whole scenarios, which must be scaled [10], recent research activities in the framework of OECD/NEA international projects have included counterpart testing among facilities with different reference reactor, scaling methodology and structure shape via the ROSA/LSTF, PKL and ATLAS Programs. In these experiments, direct extrapolation of thermal-hydraulic parameters is prevented since differences in scale involve some distortion. Nevertheless, the sequence of events is qualitatively similar in the evolution of the same transients, conditioned to a proper definition of initial and boundary conditions. Thus, counterpart experiments between different scale facilities are limited in scope but provide a valuable database for addressing scaling issues. A 1.5% SBLOCA in a hot leg with accident management measure based on Core Exit Temperature (CET) was performed in the OECD/NEA PKL-2 framework as a counterpart to a previous test belonging to ROSA-2 Project [11]. The experiment was focused on the CET analysis and questioned its use as a valid criterion to predict the Peak Cladding Temperature (PCT) since the temperatures and their correlation (CET-PCT) differed between both facilities [12] [13]. A 1% SBLOCA in a cold leg (SB-CL-32) in the LSTF was utilized to stabilize the initial and boundary conditions to the equivalent tests in PKL and ATLAS. In that test, the PCT and the core quench were heavily influenced by the loop seal clearing phenomenon, which evolves differently because of the intermediate leg geometry and the location of the active core [14] [15]. The limited knowledge on intermediate breaks led the USNRC in 2005 to propose these scenarios as a design basis event for the assessment of the effectiveness of emergency core cooling systems. This motivated two IBLOCA tests in ATLAS (13% and 17% break in a cold leg) that were conducted as counterparts to those existing in LSTF. The set comprised of the four tests provides a valuable database to investigate the ‘cliff-edge effect’ on the PCT during the IBLOCA scenario. Detection of wall thinning and cracks in the vessel head at the Davis Besse reactor in 2002 has led to conduct experiments with similar consequences to those of that scenario. Up to four tests simulating an upper head SBLOCA (0.5-1.9% cold leg area)

together with partial failure of the ECCS have been part of LSTF Programs and SB-PV-07 Test (1% SBLOCA) has been part of benchmark activities with B5.1 ATLAS test [16][17].

These experiments showed evident discrepancies in the extrapolation of results, depending on the type of scenario and the scalability of the major phenomena. In the IBLOCA tests, the mass flow discharged through the break governs the depressurization of the primary system and the major events and chronology can be preserved in ATLAS and LSTF with a proper design of the break unit. However, during the SBLOCA in the upper head, the thermal-hydraulic parameters such as pressure and temperature evolved similarly in magnitude, but all the events (trip of safety systems or excursion of the PCT) in LSTF are forward. This distortion has been mainly attributed to the design of the vessel specific to each technology.

With the same philosophy as the previous experiments, this work focuses on the analysis of a counterpart experiment between the ATLAS and LSTF facilities through simulations and distortions quantification. The scenario at issue is based on Test A1.1 in the OECD/NEA ATLAS Project [18], which reproduces a station blackout sequence with delayed and asymmetric auxiliary feedwater injection. The choice of the test is based on its potential to study the scaling of the natural circulation, given the relevance of the phenomenon in this and other accidents. Furthermore, a novel counterpart procedure is proposed, in which for the first time ATLAS acts as the prototype facility and the initial and boundary conditions of its test are scaled to obtain the equivalent ones in LSTF.

The paper is organized as follows: Section 2 describes briefly the LSTF and ATLAS facilities and their respective models built with the TRACE5 code. Furthermore, it presents the experiment under consideration and the scaled conditions of its counterpart. Section 3 summarizes the simulation results for both tests and describes the main similarities and differences. In section 4, the scalability and distortion for this test are quantified developing a global system response analysis. Section 5 summarizes the conclusions of this work.

Nomenclature

A	area
Cp	fluid heat capacity
Dh,d	hydraulic diameter
f	friction factor
g	gravity constant
h	enthalpy
H	total height
k	conductivity
L,l	length
$\dot{m}$	mass flow rate
M	total mass
P,p	pressure
$\dot{q}$	heat transfer
t	time
T	temperature
u	velocity
V	control volume
Δ	difference
δ	conduction depth
μ	specific internal energy
ρ	density
τ	residence time
υ	specific volume
$\Xi_{x,y}$	dimensionless group of a property x that changes due to a property y

Subscripts

0	reference
l	liquid-phase
m	mixture-phase
R	Ratio
v	vapor-phase

Acronyms

ATLAS	Advanced Thermal-hydraulic Test Loop for Accident Simulation
CT	Counterpart Test
CET	Core Exit Temperature
DBA	Design Basis Accident
DEC	Design Extension Conditions
ECCS	Emergency Core Cooling System
HTC	Heat Transfer Coefficient
HTSTR	Heat Structure
IBLOCA	Intermediate Break LOCA
ITF	Integral Test Facility
JAEA	Japan Atomic Energy Agency
JAERI	Japan Atomic Energy Research Institute
KAERI	Korea Atomic Energy Research Institute
LOCA	Loss Of Coolant Accident
LSTF	Large Scale Test Facility
MSIV	Main Steam Isolation Valve
MSSV	Main Steam Safety Valve
NC	Natural Circulation
NPP	Nuclear Power Plant
PCT	Peak Cladding Temperature
POSRV	Pilot-Operated Safety Relief Valve
PRZ	Pressurizer
PWR	Pressurized Water Reactor
ROSA	Rig Of Safety Assessment program
RPV	Reactor Pressure Vessel
SBLOCA	Small Break LOCA
SBO	Station Blackout
SG	Steam Generator
ST	Similar Test
USNRC	U.S. Nuclear Regulatory Commission
TLFW	Total Loss of Feedwater
TRACE	TRAC/RELAP Advanced Computational Engine

2 METHODOLOGY

2.1 ATLAS and LSTF facilities and models

ATLAS is an experimental test facility designed to reproduce the thermal-hydraulic behavior of reactors APR 1400 and OPR 1000 during the major Design Basis Accidents (DBAs) [19]. Since its launch in 2006, the extensive experimental programs have provided a valuable database including Loss of Coolant Accident (LOCA), Station Blackout (SBO) or Total Loss of Feedwater (TLFW) scenarios, and other Design Extension Conditions (DEC). The facility adopts the Reduced-Height, Full-Pressure proportions and the Ishii and Kataoka three-level scaling methodology was applied in the design to preserve the transient response of the main thermohydraulic variables and reduce the scaling distortion. Furthermore, the scales 1/2 in height, 1/144 in area and 1/288 in volume were selected to prioritize the reproduction of multidimensional behaviors and asymmetric phenomena, while reducing construction costs. As a result of the reduced height criterion, the timescale ratio is $1/\sqrt{2}$ and the duration of the experiments is $\sqrt{2}$ faster than expected on the APR1400. The maximum design pressure and temperature are 18.7 MPa and 643 K, respectively, and consequently, when using water as the working fluid, the properties of the coolant in the reference reactor and ATLAS are similar. The facility consists of a primary system with a loop configuration equal to that of the APR1400, a secondary system, safety and auxiliary systems, a power supply system, and most of the features of the IV generation reactors. The primary system is made up of the vessel, two coolant loops and a pressurizer. Each of the loops is composed of a hot leg through which the coolant flows from the vessel to the steam generator, a U-tube bundle, two-loop seals, two centrifugal pumps and two cold legs. The core power in the reference PWR is simulated utilizing 396 electrically heated rods with the capability to supply 2.15 MW (11% of the scaled power). The secondary system consists of two steam generators, their steam lines, a feedwater system, and one condensation and refrigeration loop.

The Large Scale Test Facility (LSTF) replicates the primary and secondary systems of the Tsuruga II NPP, a 4 loop Westinghouse-type reactor with 3423 MW thermal power. It was designed by the Japan Atomic Energy Research Institute (JAERI), currently Japan Atomic Energy Agency (JAEA), within the framework of the ROSA-IV (Rig of Safety Assessment - IV) program in 1985 [20]. The facility is designed based on a Full-Height, Full-Pressure configuration so that it preserves the same height and operating pressure as its reference power plant, and the scaling approach follows the Power to Volume methodology with a scaling factor of 1/48 for both parameters. Thus, its components are scaled 1/1 in height and 1/48 in areas and volumes, except the hot and cold legs. Since the four primary loops of the reference reactor are lumped into two equal volume loops, these pipes are scaled by a factor of 1/24 in area and the relation of the length to the square-root ($L/\sqrt{D}$) is preserved [21]. LSTF consists of the typical primary and secondary systems of a PWR. The primary system comprises a pressure vessel, two symmetric loops, a pressurizer and a full Emergency Core Cooling System (ECCS), and each loop includes a hot leg, a U-tube bundle, a loops seal, one pump and a cold leg. The power supplied by the core is limited to transfer 10 MW (14% of the reference scaled power) through 1008 heated rods. The secondary system consists of two steam generators and their main and auxiliary feedwater pumps.

The ATLAS and LSTF models developed with the TRACE5 thermal-hydraulic code [22] deal to faithfully reproduce the thermal-hydraulic behavior of the facilities. To this end, their technical specifications are adapted to the modeling code options, paying special attention to the nodalization of the models. Figure 1 shows the nodalization sketches of the ATLAS and LSTF models using the Symbolic Nuclear Analysis Package (SNAP) software. The ATLAS model consists of 76 hydraulic components (1 VESSEL, 53 PIPE, 1 PRIZER, 4 PUMP, 2 SEPARATOR, 2 TEE, 7 VALVE, 3 FILL

and 5 BREAK). For its part, the LSTF model consists of 81 hydraulic components (1 VESSEL, 23 PIPE, 1 PRIZER, 2 PUMP, 22 TEE, 14 VALVE, 11 FILL and 7 BREAK).

The models have common characteristics. The vessels are modeled using a VESSEL-3D component to allow the simulation of multidimensional phenomena. Both include an annular downcomer, lower plenum, a nucleus, upper plenum, and upper head, however, their nodalization differs between them. The loops, U-tube bundles, injection lines, accumulators, as well as steam generators, are modeled using PIPE components. The roughness of the wall set for all of them is 5E-5 m, as it is considered a common value in stainless steel pipes. The U-shaped tube bundles are made up of 176 tubes in ATLAS and 141 tubes in LSTF, distributed among different levels, so to simplify the models, the bundles are grouped into one PIPE component. These PIPEs preserve the inlet and outlet temperature, pressure drop, and heat transfer through the wall of the original tubes. The pressurizers are modeled by a PRIZER component, which is connected to a hot leg through a PIPE which represents the surge line.

The core power is supplied by POWER components, which lend the power to the electric rods modeled with cylindrical HEAT STRUCTURE (HTSTR) components. Each heat structure represents the set of heaters located in given nodes (ring and sector) of the vessel. Similarly, HTSTRs replicate the heat transfer processes through the tube bundles in the steam generators and the heat losses. The heat transfer between the primary and secondary systems is modeled simultaneously associating a HTSTR to a tube bundle and the evaporator of the steam generator. Heat losses in experimental facilities are decisive in the calculation of the net power of the system and therefore in the evolution of accidents in which natural circulation is a dominant phenomenon [23] [24]. Thus, it is necessary to reproduce them to correctly simulate these transients using HTSTRs that act as a boundary condition between the facility and the environment. Specifically, the heat losses in the hot and cold legs, in RPV and SG vessels, and also in the pressurizer are modeled as the condensation of steam in the PZR can play an important role on the transient. Heat losses to the environment in ATLAS and LSTF have been quantified through separate effect heat loss tests consisting in cooling transients [19][25]. In order to evaluate the heat losses with the TRACE5 code, the most widely used technique by the modelers rely on selecting heat transfer coefficients (HTC) [W/m^2K] for each facility component. This has been done through sensitivity analysis on the HTCs, so that the simulation of these tests achieves the highest accuracy.

Moreover, FILL components simulate the feedwater systems and the ECCS, and the set of a VALVE and a BREAK the boundary conditions downstream the safety and relief valves.

The experimental test facilities are highly instrumented for the measurement of temperatures, static and differential pressures, flow rates or liquid level. In TRACE5 models, this function is performed by SIGNAL VARIABLE components. Furthermore, to control safety systems and establish accident management measures, CONTROL BLOCK and TRIP components process the signals.

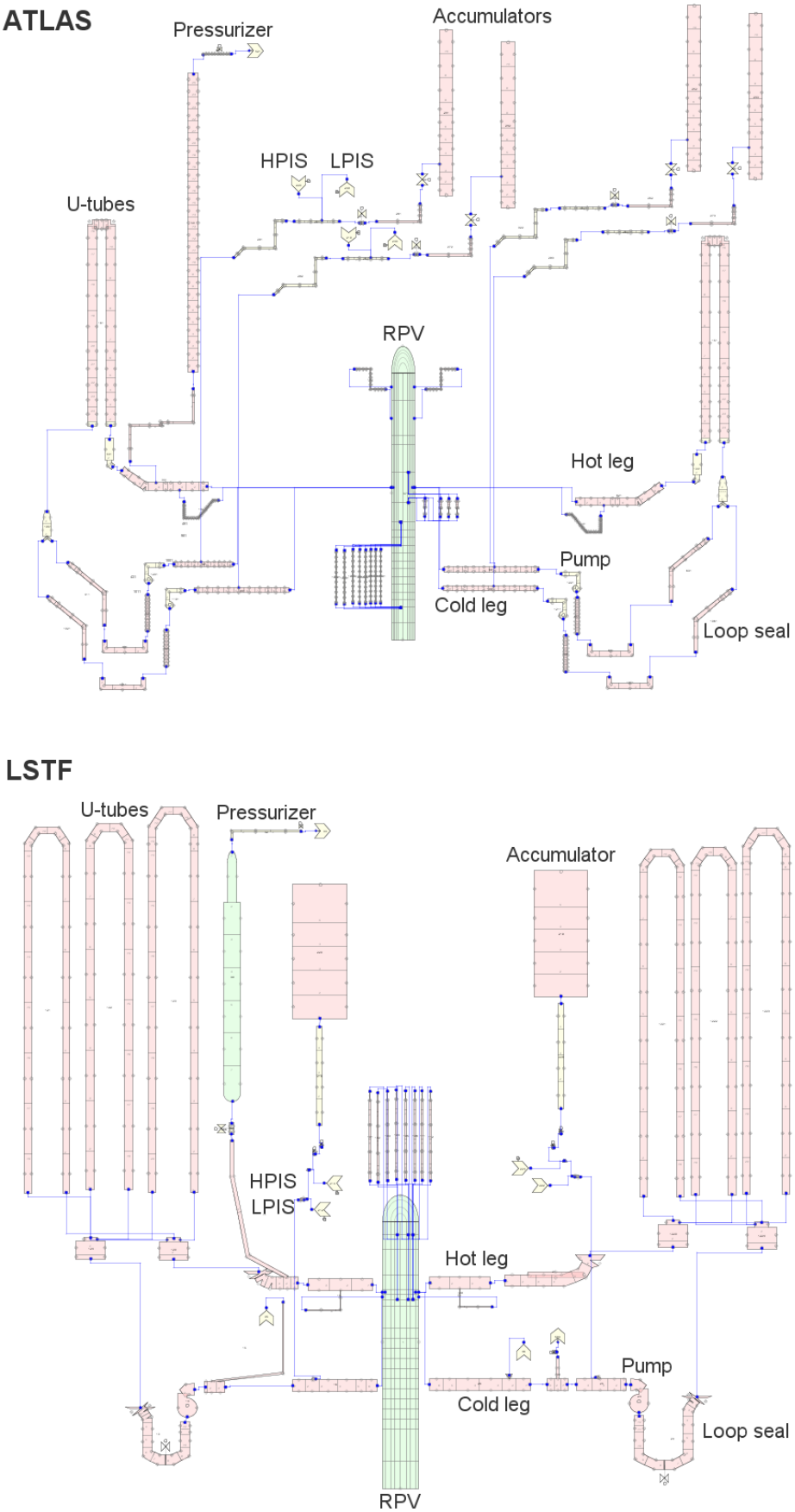

Figure 1: Nodalization sketches of ATLAS and LSTF.

2.2 Test conditions

2.2.1 Test A1.1 in ATLAS facility

After the Fukushima accident, beyond design basis events have been a subject of international research for the reinforcement of nuclear safety. Thus, KAERI (Korea Atomic Energy Research Institute) has included DEC such as station blackout (SBO) and Total Loss of FeedWater (TLFW) into the experimental programs at the ATLAS facility [26].

Test A1.1 was carried out in ATLAS on October 28, 2014, with the objectives of studying high-pressure asymmetric single- and two-phase natural circulation flow characteristics and the effects of cooling during a Station Blackout (SBO) accident [18]. This event refers to the total loss of offsite alternating current along with the failure of all diesel generators so that the active safety systems become unused. This experiment in particular reproduces a Station Blackout scenario with asymmetric and delayed feedwater supply to one steam generator to enable the cooldown.

The initial test conditions of pressure in the pressurizer (PRZ), core exit temperature and mass flow in the hot legs are 15.5 MPa, 598 K and 4 kg/s, respectively, according to the test specifications. The initial core power was pre-determined to supply 1.56 MW in addition to heat losses (about 80 kW) with a uniform radial power distribution and the chopped cosine shape for the axial power profile. After reaching a steady-state, the test initiates with the reactor trip and the core power decreases following 1.2-times the ANS-73 decay curve [18]. Immediately, the reactor coolant pumps stop, the feedwater supply interrupts, and the main steam valves close. When the steam generators remain isolated the secondary pressure tends to increase until the main steam safety valves (MSSV) opening set value, and inventory is gradually drained. The globe-type valves, whose flow area is 0.000346 m2, are designed to open and close at 8.1 MPa and 7.7 MPa, respectively. As the steam generators empty, the heat transfer through U-tube bundles degrades and the primary system pressure and temperature increase. Likewise, the primary system inventory is discharged through a pilot-operated safety relief valve (POSRV) placed at the top of the pressurizer. The POSRV flow area is 0.000207 m^2 and the setpoint pressures for opening and closure are 17.03 MPa and 14.82 MPa in the pressurizer. Since heat losses from the PRZ are usually compensated due to their influence on the evolution of prolonged transients, a proportional heater supplies 16.36 kW at constant power from the start of the test until the first opening of the POSRV.

When the core uncovers, and the peak cladding temperature reaches 723 K, the auxiliary feedwater system activates. Recovering the feedwater supply in the steam generator coupled to the loop with pressurizer, a flow rate of about 0.198 kg/s is pumped intermittently to keep the water level in the device in a range between 25% and 40%.

2.2.2 Test conditions for counterpart in LSTF

ATLAS and LSTF concepts are based on different reference reactors and similarity laws and thus the design of mutual counterpart and similar tests must be supported on a scale analysis between both facilities. Additionally, when the facilities differ in their design in height, as is the case, it must be considered if this fact is limiting in terms of scalability of results.

Reduced height facilities having an aspect ratio closer to the prototype than a full-height facility can better preserve multi-dimensional phenomena in the reactor pressure vessel. By contrast, the preservation of local phenomena as critical heat-flux, flow stagnation or reflooding might be difficult because of their dependence on the height of the components, but the distortion introduced by the

effect of height scaling is not significant compared to deficiencies in the scaling of the boundary conditions [27]. The reduced height scaling also results in the distortion of time, advancing the chronology of the main events of the transients. This makes reduced height test facilities appropriate for conducting slow and prolonged scenarios such as SBLOCA for better preserving the phenomenology. Likewise, stored energy in the structures and heat losses have a strong impact on reduced test facilities and contribute to temporal distortion but have the opposite effect. Despite distortion of the chronology in ATLAS, tests for the characterization of natural circulation have shown similar behavior to that expected in a typical PWR [19] and, since it is the figure of merit of the experiment under study, the facility is considered suitable for the purpose of this work.

To establish the initial and boundary conditions for a test in which a facility takes the role of a prototype system and the other that of a model, the most appropriate similarity laws to relate the thermal-hydraulic behavior of the ITFs should be applied.

The difference in height between the facilities and their operating mode after the reactor shutdown during accidental scenarios make the similarity criteria for two-phase flow in natural circulation derived by Ishii and Kataoka [28] the most suitable for planning the counterpart transients. These similarity laws were obtained from the integral effects of the two-phase flow balance equations along a closed-loop and using the perturbation method based on the drift-flux model developed by Ishii and Zuber [29] and Ishii and Jones [30]. In this way, the model prioritizes the response of the whole mixture instead of the two phases separately. Thus, the similarity between the processes in a prototype and a model can be achieved if the dimensionless groups derived from the scaling criteria (Zuber, Sub-cooling, Froude, Drift flux, Friction, Orifice, Time and Thermal Inertia) are the same in both systems.

In the particular case that the prototype and model facilities operate with the same fluid under the same pressure and temperature conditions, it can be considered that the properties of the fluid are the same in both systems.

$$\rho_R = \rho_{gR} = C_{pR} = k_R = \mu_R = \mu_{gR} = \Delta h_{fgR} = 1 \quad (1)$$

Under these conditions, the similarity criterion for the Froude number is simplified as:

$$(N_{Fr})_R = \frac{u_R^2}{l_R} = 1 \quad (2)$$

And

$$u_R = \sqrt{l_R} \quad (3)$$

The similarity criterion for the phase change number (Zuber number) results:

$$\left(N_{pch}\right)_R = \frac{\delta_R q_R l_R}{d_R u_R} = 1 \quad (4)$$

This equality implies that:

$$\frac{\delta_R}{d_R} = 1 \quad (5)$$

The previous relation is not fulfilled between ATLAS and LSTF in major components and consequently, the phenomena influenced by the conduction depth (δ) will be distorted. Specifically, the quotient δ_R/d_R is equal to 0.64 in the hot legs, 0.73 in the cold legs and 1.3 in the downcomer of the vessel. On the other hand:

$$\frac{q_R l_R}{u_R} = 1 \quad \text{and} \quad q_R = \frac{u_R}{l_R} = \frac{1}{\sqrt{l_R}} \quad (6)$$

Besides, the time ratio number yields the chronological relation of the phenomena in each ith section:

$$(N_t)_{R,i} = \left(\frac{l_R}{u_R}\right)_i = \sqrt{l_R} \quad (7)$$

The strategy to determine the counterpart test conditions in LSTF from those in ATLAS is based on the application of previous similarity criteria. The first step consists of comparing geometric aspects (lengths, areas and volumes) that characterize both the components and the facilities as a whole. Among them, two major independent parameters are selected to calculate the scaling ratios. To preserve natural circulation characteristics in the loops, the parameters are the height difference between the active core and the SG U-tube and the primary system inventory. By this way, the length ratio (l_R) is equal to 9.13 m/19.54 m=0.47 and the volume ratio ($l_R d_R^2$) is 1.64 m^3/8.14 m^3=0.2. When using this pair of parameters, the scaling ratio of diameter (d_R) is 0.65 and the rest of the dependent scaling ratios in Table 1, like core power, time or flow rate, are computed. The pressure and temperature ratios equal to 1 are required to preserve these parameters meet equal fluid conditions in both systems.

Table 1: Scaling ratios between ATLAS and LSTF

Parameter	Similarity ratios	ATLAS/LSTF ratios
Length	l_R	**0.47**
Diameter	d_R	0.65
Area	d_R^2	0.43
Volume	$l_R d_R^2$	**0.2**
Core ΔT	T_R	1
Pressure	P_R	1
Heat flux	$l_R^{-1/2}$	1.46
Core power	$l_R^{1/2} d_R^2$	0.29
Power/Volume	$l_R^{-1/2}$	1.46
Flow rate	$l_R^{1/2} d_R^2$	0.29
Velocity	$l_R^{1/2}$	0.68
Time	$l_R^{1/2}$	0.68

As a counterpart test of the A1.1 experiment in ATLAS, the initial and boundary conditions are established from those in the target scenario.

According to the power scaling ratio, $l_R^{1/2} d_R^2$, the initial power in LSTF should be 5.4 MW distributed in a uniform radial direction and the chopped-cosine shape for the axial profile in the heater rods. However, the core power is increased to the LSTF rated value, 10 MW, distributed in 3 groups (1786 kW, 3572 kW and 4642 kW) to achieve equal pressure and temperature conditions at the initial steady state. Once the core is tripped at the beginning of the test, the power in LSTF results from directly scaling the decay curve in ATLAS with a factor of 1/0.29. Even though the power defined in LSTF for performing the steady-state is approximately double that postulated by the scaling methodology, this correction enables reaching the target pressure and temperature conditions without affecting the evolution of the experiment. In addition to the core power, the heater rods in the vessel and the pressurizer heaters must compensate for the heat losses to the environment. Therefore, the proportional heaters supply 5 kW until the first opening of the POSRV.

The scaling of available inventory is decisive in the reproduction of natural circulation performance. On this account, the liquid level in the pressurizer of LSTF is tuned to 7.25 m to scale the total amount of coolant in the primary system as an initial condition. Once the experiment is started, the increase of

pressure triggers the safety valves opening. The mass flow rate through the valves is determined by scaling their flow area by a ratio d_R^2=0.43. The flow area for the MSSVs is adjusted to 0.0008 m^2, and that for the POSRV is 0.00048 m^2. As the same conditions as in the ATLAS test, the pressures for the opening and closing of the valves are preserved and they are respectively 8.1 MPa and 7.7 MPa in the MSSVs and 17.03 MPa and 14.82 MPa in the POSRV.

In the A1.1 Test, the auxiliary feedwater is actuated when the core is uncovered and the peak cladding temperature reaches 723 K. The counterpart test in LSTF uses the same setpoint temperature to activate the accident management measure and, as required by the global scaling ratios, the flow rate of 0.68 kg/s is supplied to one steam generator.

2.3 Global system scaling analysis

Based on the simulation results of the counterpart test, a global system scaling analysis is developed to justify the similarity of thermal-hydraulic behaviors between the facilities and to identify the parameters and phenomena that produce differences taking place during the test. Specifically, the analysis focuses on the natural circulation phase of the test, as it is the most relevant in the evolution of an SBO-type accident. The proceed methodology is the dimensionless analysis performed in the top-down scaling, also known as global system scaling, of some of the relevant scaling methodologies [3]. The top-down scaling ensures the preservation of the transient response of major variables evaluating the global system behavior and system interactions. Besides, the methodology is applied to achieve the derivation of dimensionless groups governing similitude between different scale systems and identifies scaling distortions. This scaling approach has been usually used to quantify the scalability of the thermal-hydraulic phenomena in the experimental facilities and their respective reference reactors over a single transient [31] [32]. However, the appliance of the same approach to the analysis of a counterpart test between the pair of facilities ATLAS/LSTF has also assessed the similarity of the transfer processes (mass, enthalpy, heat flux and volumetric flow) in a LOCA transient [33].

This analysis procedure reduces the variables involved in a physical phenomenon to a set of dimensionless monomial groups that describe it with the same precision as the initial approach, only with fewer variables. Furthermore, if a law relating dimensional variables is equivalent to one non-dimensionalized, the second law is also fulfilled at other scales. These enable comparing processes and phenomena in driving the response of diverse facilities.

In the scaling approach, the first step divides the hydraulic transient into time intervals, or phases, based on phenomenological considerations. The evolution of each phase can be described from the three conservation equations (mass, energy and momentum). Next, the conservation equations are combined with constitutive equations (equations of state and thermodynamic relations) to build the model that governs the significant processes, e.g. a pressure rate equation [34]. The model can be normalized and the coefficients of the non-dimensional equations are expressed in terms of π-monomial groups, $\Xi x,y$, which indicate the relative importance of a parameter y in the changes of a parameter x. Therefore, if the phenomenon at issue, $\dot{x}$, involves several transfer processes ($\Xi\dot{x},y_1$, $\Xi\dot{x},y_2$, …, $\Xi\dot{x},y_n$), the dimensionless groups can be compared to rank their contribution to the event. That is, the numerical value of the groups establishes the hierarchy of their importance. Then, a process is considered important if the associated π- group is greater than 1/10 of the largest π- group [31].

The criterion to evaluate the distortion in the scaling analysis relates the dimensionless groups of two facilities. Since the groups are derived from fixed geometrical parameters and operating variables at reference conditions, they are constant and there is only one group for each transfer process. Hence, the ratio between the groups of both systems representing the same phenomenon indicates the degree of correlation or distortion. In respect of this ratio, a value close to 1 indicates similarity. For this criterion Wulff, W. [35] establishes three ranges to qualify the distortion:

Phenomenon well-scaled $\frac{1}{2} < \frac{\Xi x,y\ Facility}{\Xi x,y\ Prototype} < 2$

Noticeable scaling distortion $\frac{1}{3} < \frac{\Xi x,y\ Facility}{\Xi x,y\ Prototype} < \frac{1}{2}$ or $2 < \frac{\Xi x,y\ Facility}{\Xi x,y\ Prototype} < 3$

Significant scaling distortion $\frac{\Xi x,y\ Facility}{\Xi x,y\ Prototype} < \frac{1}{3}$ or $\frac{\Xi x,y\ Facility}{\Xi x,y\ Prototype} > 3$

If the π-groups have a different sign, the ratio $\frac{\Xi x,y\ Facility}{\Xi x,y\ Prototype}$ is lower than 0 and the phenomenon is completely distorted.

The application of this methodology is aimed at clarifying some causes of the correspondence or the important differences between the ATLAS and LSTF behavior depending on the counterpart test. Then, the analytical study may enhance confidence in counterpart tests as a technique to address the scaling issue.

3 RESULTS

The current section includes the results of the most relevant thermal-hydraulic parameters in the A1.1 experiment in ATLAS, its simulation with the TRACE5 code and the simulation of the proposed counterpart test in LSTF. For both simulations to be comparable, the LSTF results are shown scaled according to the ratios between the two facilities. First, a steady state was simulated with both models to validate the initial and boundary conditions. Table 2 presents relative errors (%) in ATLAS parameters, and those in LSTF, regarding their target conditions for Test A1.1. As can be seen, initial condition errors in both simulations are less than 6%.

Table 2: Initial test conditions

Parameter	ATLAS simulation rel. error	LSTF simulation rel. error
Power (MW)	0	0
Pressurizer pressure (MPa)	0.3	0.2
Core inlet temperature (K)	0.6	0
Core outlet temperature (K)	0	0
Mass flow rate - hot leg (kg/s)	1	0.7
Steam flow rate (kg/s) (SG1)	4	6
Steam pressure (MPa)	0	0
Secondary side level (m)	3.4	2

Table 3 summarizes the sequence of the major events observed in all three cases and a significant discrepancy is evidenced in the chronology. The reduced-height design of ATLAS involves the scaling of times by a factor of 0.72, or in other words, that events in ATLAS should occur 1/0.72 times faster

than in LSTF. Then, scaling the times should lead an equivalent chronology. The major events in Table 3, far from being simultaneous in both facilities, occur well in advance in LSTF. This difference is attributed to the characteristics of natural circulation, specifically the net power and the distinctive flow path in each facility determine the natural circulation mass flow rate along the loops.

Table 3: Chronology of major events

Event	Experiment [s]	ATLAS simulation [s]	Scaled LSTF simulation [s]
Start of test	0	0	0
MSSV first opening	12	12	11
SG dry out	5590	5556	3955
1st POSRV opening	6448	5715	3112
NC ending	8188	8620	7000
Pressurizer full	8302	7761	4071
AFW supply	11095	11046	6395
End of test	15000	15000	15000

The test starts with the stop signal for all active components of the facility and the turbine trip. Due to the isolation of the steam generators, the secondary pressure increases rapidly up to 8 MPa and causes the main steam safety valves (MSSV) to open and close periodically to control pressure. Since the primary system temperature is higher than the secondary one, decay heat is transferred to the steam generators (SG) while secondary inventory boils and the gas mass flow is discharged. Hence, the liquid level gradually decreases until the steam generators dry out. As seen from Figure 2, the steam generators in LSTF empty previously. Since the initial inventory is scaled according to the volume global ratio, this results from a higher vaporization rate. Once the SGs become empty, the experimental secondary pressure decreases linearly despite the MSSV remain close, which is attributed to leakages in the valves [18]. This effect is not appreciated in the calculations because unquantified leakages are not modeled in the code.

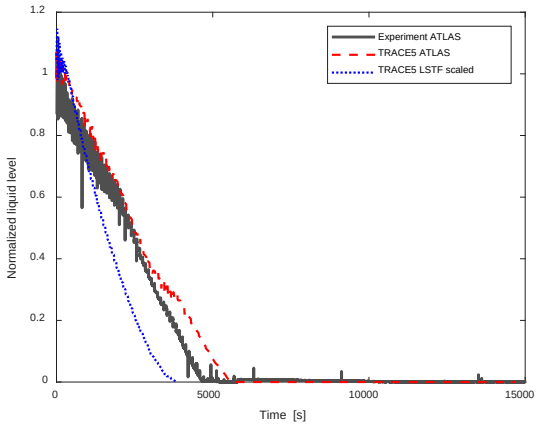

Figure 2: Liquid level in non-cooled steam generator.

From the beginning of the transient, the natural circulation flow is quite effective in removing heat from the core however, the primary system pressure increases slowly until reaching the POSRV opening value. Then, coolant is discharged through cyclic apertures while the primary pressure ranges

between 17.03 MPa and 14.82 MPa, which causes a noticeable loss of coolant. Although the code predicts reasonably well the overall trend of the pressure, differences among the three data series appear in Figure 3. The first POSRV opening in ATLAS simulation is slightly anticipated to the experiment but that in LSTF occurs much more advanced. It is also worth noting that as an effect of a higher pressurization rate in LSTF, the POSRV openings are more frequent than in ATLAS.

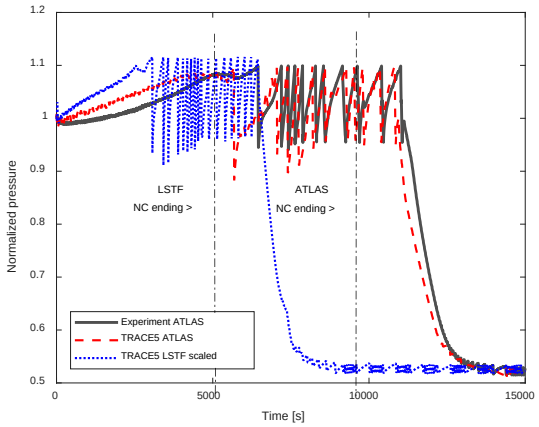

Figure 3: Primary pressure.

At the time of the core shutdown, the mass flow rate along the loops decreases rapidly and natural circulation (NC) favored by the core power decay is established. Long-term single-phase NC is held until voiding forms in the hot leg. TRACE5 simulates properly the overall trend of NC mass flow in ATLAS, as shown in Figure 4a and Figure 4b. The mass flow rate is exactly reproduced until the NC interruption, which happens simultaneously in the experiment and the simulation. The NC mass flow rate differs from ATLAS to LSTF. During the steam generators draining and until the POSRV 1st opening, the mass flow in ATLAS is slightly higher, which is justified by a discrepancy of about 8 K in the core exit temperature. The difference in temperatures increases the heat transfer through the U-tube bundles, advances the steam generators dry out and distorts the chronology of events in LSTF. Both the power scaling technique for the purposed scenario in LSTF, and mainly the different geometric configurations of the loops and the vessels, may induce this distortion.

After consecutive discharges through the POSRV, the primary system drains, the saturated conditions become at the hot legs and U-tube bundles, and natural circulation flow terminates. Just before, the scaled mass flow in LSTF is equalized with that in ATLAS. Shortly after, loop seal clearing occurs in one intermediate leg of the ATLAS experiment and simulation, but this only briefly restores the core liquid level. This phenomenon is not predicted with the LSTF model. After the auxiliary feedwater injection into one steam generator, experimental mass flow shows asymmetric behavior between two loops. In the loop without pressurizer, a small amount of steam condenses in the U-tubes with reflux formation. On the contrary, the natural circulation flow is recovered in the cooled loop as the auxiliary feedwater system refills the steam generator and the heat removal capacity is restored. TRACE5 code does not reproduce the asymmetric behavior with any of the models and only a very low stratified flow is identified (Figure 4b).

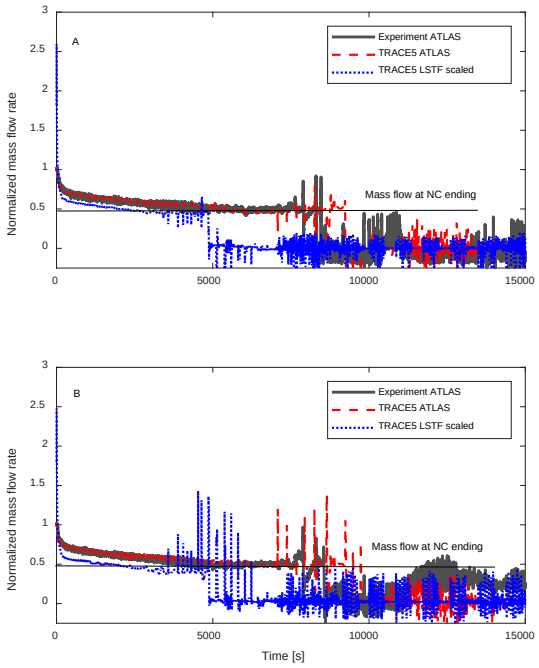

Figure 4: Mass flow rate a) Loop without pressurizer b) Loop with pressurizer

At the beginning of the experiment, the liquid level in the pressurizer decreases, but when the steam generators dry out, heat transfer through U-tube bundles degrades, the water level changes its trend and increases sharply by the volumetric expansion of coolant (Figure 5). Then, the upper plenum of the vessel reaches saturated conditions and takes over momentarily the pressurizer function i.e. the pressurizer provides only the function of a buffer tank and the vessel behaves like a pressurizer. As can be seen in Figure 5, the initial collapsed liquid level in the pressurizer differs between the facilities. As mentioned in the design of the test for LSTF (Section 2.2.2), the scaling of the total inventory in the primary system was considered a priority over the liquid level in the pressurizer. The maximum liquid level in LSTF is lower than that of ATLAS due to the lower height of its pressurizer.

The ATLAS and LSTF vessel design exhibit differences that directly affect the inventory distribution and the evolution of the transient. More specifically, the upper plenum plate in ATLAS (separation from the upper head) has perforations, while in LSTF this plate does not enable the flow path between both regions. Thus, in ATLAS, the upper plenum and the upper head become saturated at once and act as a single volume. As the POSRV releases a larger coolant flow, the liquid level decreases drastically and leads to the core uncovering. In LSTF simulation, a certain amount of water that would delay the core heat up is retained in the upper head. When the auxiliary feedwater injection activates, the liquid level in the vessel of both facilities increases and the cores are quenched. Figure 6 shows the collapsed liquid level in the Reactor Pressure Vessel (RPV).

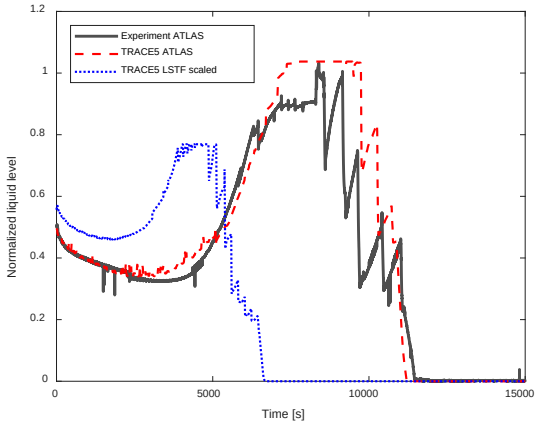

Figure 5: Collapsed liquid level in the pressurizer.

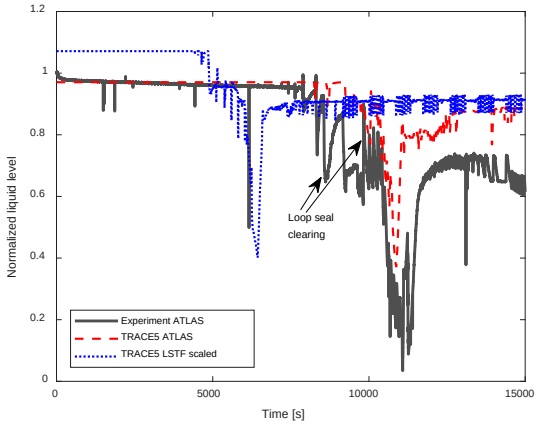

Figure 6:Collapsed liquid level in Reactor Pressure Vessel.

The cyclical performance of the POSRV to control the primary pressure causes the discharge of a large quantity of coolant. Figure 7 shows the integrated mass flow through the valve, in which the steps correspond to a liquid loss in each opening. Although the 1st opening in the ATLAS simulation is ahead of the experiment (Figure 3), the liquid discharged is practically simultaneous in both cases. When the POSRV is permanently closed, the code overestimates the amount of lost inventory and therefore the collapsed liquid level in the vessel at the end of the transient is slightly higher, as can be seen in Figure 6 from 12500 s. In accordance with other parameters, the steeper growth curve in LSTF is advanced.

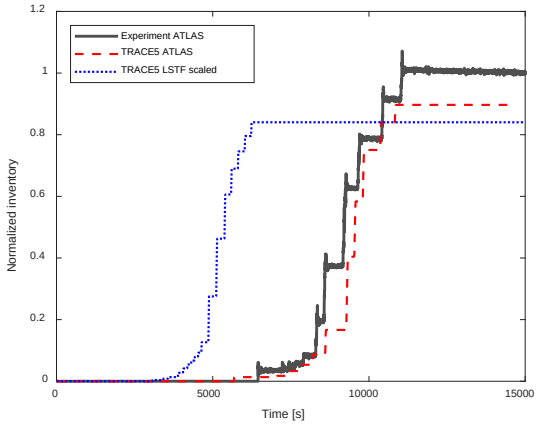

Figure 7:Discharged inventory through the POSRV.

The peak cladding temperature (PCT) is the figure of merit or primary safety criteria for taking accident management actions in Test A1.1 The core uncovering causes a fast excursion of the PCT and when the temperature reaches 723 K the auxiliary feedwater system is activated. Then, the PCT continues to increase abruptly for few minutes and decreases equally quickly due to the effect of coolant injection in the steam generator. Thus, the asymmetric feedwater supply proves to be a very effective measure to rapidly restore the core level and reduce the PCT. The experimental and simulated PCT in ATLAS are drawn together with that of LSTF in Figure 8. The accurate simulation of the PCT in ATLAS is remarkable, the excursion occurs at the same time as in the test and reaches the same maximum value. The PCT in LSTF behaves equivalently to ATLAS, but the excursion is not so sharp because the whole core is quenched earlier due to faster recovery of the core liquid level.

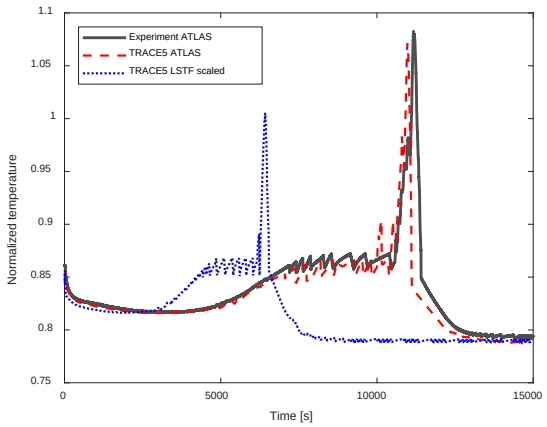

Figure 8: Peak cladding temperature.

4 SIMILARITY ANALYSIS ON NATURAL CIRCULATION PHASE

During a station blackout accident, all active safety systems are disabled but despite this circumstance, several studies have demonstrated natural circulation flow to be capable of removing decay power. Therefore, exhaustive knowledge of this phenomenon and its correct prediction is relevant in the nuclear safety field.

The natural circulation phase in Test A1.1 covers the period in which a coolant flow is held in the loops due to natural convection, that is, heat transport from a heat source (the core) to a heat sink (the steam generators). According to the pressure system behavior, natural circulation phase may be split into two stages as represented in Figure 9. The first one runs from the pumps stopping to the first opening of POSRV. During that stage, the pressure increases slowly until reaching the valve opening value. At that moment, the second stage begins and lasts until the mass flow interruption in the loops. Over this stage, the POSRV opens and closes repeatedly, and the primary pressure fluctuates between the valve set points.

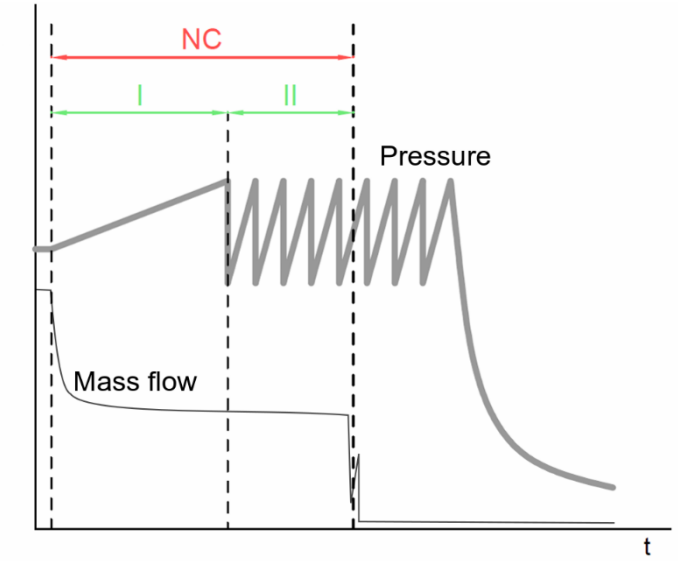

Figure 9: Natural circulation stages.

The global system scaling analysis draws from the evaluation of the conservation equations. In order to model the thermal-hydraulic behaviors through the mass and energy equations, the whole primary system is simplified to a large volume of subcooled liquid connected to another volume, the pressurizer, where liquid and gas phases coexist. In this simplified system, thermal-hydraulic equilibrium between phases is considered. Besides, the heat balance is obtained by subtracting the heat transfer to the secondary systems and the heat losses through the walls of all components from the power provided by the core and other heaters. Under these conditions, the mass and energy conservation equations for the two natural circulation stages can be written in the following forms regardless of its duration in each facility:

Natural circulation - First stage

$$\frac{dM}{dt} = 0 \quad (8)$$

$$\frac{dp}{dt} = \frac{\left(\frac{\delta p}{\delta \mu_m}\right)_{v_m}}{M}\{\dot{q}_{core} - \dot{q}_{SG} - \dot{q}_{loss}\} \quad (9)$$

Natural circulation - Second stage

$$\frac{dM}{dt} = -\dot{m}_{POSRV} \quad (10)$$

$$\frac{dp}{dt} = \frac{\left(\frac{\delta p}{\delta \mu_m}\right)_{v_m}}{M}\{-\dot{m}_{POSRV}(h_v - \mu_v) + \dot{q}_{core} - \dot{q}_{SG} - \dot{q}_{loss}\} - \frac{\left(\frac{\delta p}{\delta v_v}\right)_{\mu_v}}{M\rho_v}(-\dot{m}_{POSRV}) \quad (11)$$

The momentum balance drives the flow rate in the natural circulation phenomenon. Hence, the mass flow is derived from the evaluation of the momentum conservation equation over a closed-loop [36] comprised of a hot leg, the upward and downward sides of a steam generator, an intermediate and cold leg, and the downcomer, lower plenum, core and upper plenum of the vessel. At the same time, each component is discretized in nodes characterized by a constant area. According to simulation results, the whole loop is supposed to remain in liquid single-phase state. Based on these assumptions, the integration of the equation results as follows:

$$\sum_i \left(\frac{L_i}{A_i}\right)\frac{d\dot{m}}{dt} = \rho_l g \Delta H_{NC} - \sum_i \frac{f_i}{D_{h,i}}\frac{\dot{m}_i^2}{2A_i^2\rho_{l,i}} - \sum_j k_j \frac{\dot{m}_j^2}{2A_i^2\rho_{l,j}} \quad (12)$$

Continuing with the scaling analysis methodology, the conservation equations are normalized to derive the dimensionless groups. These terms identified to the thermal-hydraulic parameters and phenomena govern similitude between facilities. For that purpose, the following dimensionless magnitudes in Eq. (13) are defined by using reference conditions and parameters, which are measured at the meantime of each stage.

(13)

$$p^* = \frac{p}{\Delta P_0} \qquad L^* = \frac{L}{H_0} \qquad t^* = \frac{t}{\tau_0} \qquad \dot{m}^* = \frac{\dot{m}}{\dot{m}_0}$$

$$\rho^* = \frac{\rho}{\rho_0} \qquad h^* = \frac{h}{h_0} \qquad v^* = \frac{v}{v_0} \qquad \dot{q}^* = \frac{\dot{q}}{\dot{q}_0}$$

$$\mu^* = \frac{\mu}{\mu_0} \qquad t^* = \frac{t}{\tau_0} \qquad \left(\frac{\partial \mu}{\partial p}\right)_v^* = \frac{\left(\frac{\partial \mu}{\partial p}\right)_v}{\left(\frac{\partial \mu}{\partial p}\right)_{v,0}} \qquad \left(\frac{\partial \rho_g}{\partial p}\right)_{sat}^* = \frac{\left(\frac{\partial \rho_g}{\partial p}\right)_{sat}}{\left(\frac{\partial \rho_g}{\partial p}\right)_{sat,0}}$$

By substituting the dimensionless magnitudes in the mass, pressure and momentum balance equations, the equations turn into normalized (Eqs. (14), (15), (16), (17) and (18)) and yield the dimensionless groups.

Natural circulation - First stage

$$\frac{dM^*}{dt^*} = 0 \quad (14)$$

$$\frac{dp^*}{dt} = \Xi_{\dot{p},\dot{q}_{net}} \frac{\left(\frac{\delta p}{\delta \mu_m}\right)_{v_m}^*}{M^*}\dot{q}_{net}^* \quad (15)$$

Natural circulation - Second stage

$$\frac{dM^*}{dt^*} = \Xi_{\dot{M},\dot{m}}(-\dot{m}^*_{POSRV}) \quad (16)$$

$$\frac{dp^*}{dt} = -\Xi_{\dot{p},\dot{m}(h_{out}-\mu_m)} \frac{\left(\frac{\delta p}{\delta \mu_m}\right)^*_{v_m}}{M^*} \dot{m}^*_{POSRV}(h^*_v - \mu^*_v) + \Xi_{\dot{p},\dot{q}_{net}} \frac{\left(\frac{\delta p}{\delta \mu_m}\right)^*_{v_m}}{M^*} \dot{q}^*_{net} -$$

$$\Xi_{\dot{p},\dot{m}v_m} \frac{\left(\frac{\delta p}{\delta v_m}\right)^*_{\mu_m}}{M^*} \frac{1}{\rho^*_m}(-\dot{m}^*_{POSRV}) \quad (17)$$

In both stages:

$$\sum_i \Xi_{L/A} \frac{d\dot{m}}{dt} = \Xi_{Ri}\rho_l - \Xi_F \sum_i \left(\frac{f_i L_i}{2D_{h,i}} + \frac{k_i}{2}\right) \frac{\dot{m}_i^2}{\rho_{l,i}} \quad (18)$$

The computation of the groups for both facilities enables ranking the relative importance of the transfer processes and quantifying the distortion between ATLAS and LSTF. Table 4 and Table 5 summarize the scaling analysis results during the stages of the natural circulation phase. The first column lists the dimensionless groups, the second and fourth columns show the relevant values for ATLAS and LSTF, and the third and fifth ones their importance or contribution to the system evolution. The sixth column shows the distortion ratios between facilities.

Four transfer processes govern the first stage. Since the facilities remain closed, the balance of the mass flow rates entering and leaving the system is zero, and the increase in pressure is due to the net power transferred to the system. Thus, only the dimensionless group related to this process, $\Xi_{\dot{p},\dot{q}_{net}}$, is evaluated and its relative importance is one. For its part, the momentum conservation equation provides three dimensionless groups, $\Xi_{L/A}$ Ξ_{Ri} and Ξ_F. As can be appreciated from the summary of results in Table 4, the natural circulation driving force term (Ξ_{Ri}) is the dominating dimensionless group and the relative importance of the other groups is negligible compared to this one. The high value of this group (Richardson number), 3490 in ATLAS and 5880 in LSTF, indicates the insufficiency of kinetic energy to homogenize the fluid and confirms the importance of gravitational forces in natural circulation. Additionally, the group that relates the balance of the mass flow rates entering and leaving the system, $\Xi_{\dot{M},\dot{m}}$, is calculated with a value equal to one, by definition.

The Wulff criterion limits the distortion ratio to the interval [0.5,2] to consider a well-scaled phenomenon. Accordingly, all transfer processes present low distortion between facilities. It should be noted that the greatest distortions become from net heat transferred to the system and the natural circulation driving term, but their values are in the range to avoid distortion of the relevant phenomenology.

Table 4: Summary of the scaling approach results for the NC first stage.

Dimensionless groups	ATLAS groups	ATLAS importance	LSTF groups	LSTF importance	Distortion ratio
$\Xi_{\dot{M},\dot{m}} = \frac{\dot{m}_0}{M_0}\tau_0$	1.00	1.00	1.00	1.00	1.00
$\Xi_{\dot{p},\dot{q}_{net}} = \frac{\tau_0}{\Delta P_0}\frac{\left(\frac{\delta p}{\delta \mu_m}\right)_{v_m,0}}{M_0}\dot{q}_0$	-6.47	1.00	-4.39	1.00	1.47
$\Xi_{L/A} = \frac{\sum(L/A)_i}{(L/A)_0}$	28.1	0.008	23.1	0.004	1.22
$\Xi_{Ri} = \frac{g\overline{\rho_0}\Delta H}{\rho_0 u_0^2}$	3490	1.00	5880	1.00	0.56
$\Xi_F = \sum\left\{\left(\frac{f_i L_i}{2D_{h,i}} + \frac{k_i}{2}\right)\left(\frac{A_0}{A_i}\right)^2\right\}_0$	24.1	0.007	16.3	0.003	1.48

In the second stage, the pressure reaches the POSRV set point and a certain amount of coolant is discharged to prevent overpressure of the system. Thus, the equation describing the pressure evolution derives two more dimensionless groups related to the mass flow leaving the facility, $\Xi_{\dot{p},\dot{m}v}$, and its enthalpy, $\Xi_{\dot{p},\dot{m}(h_{out}-\mu_m)}$. However, given the results summarized in Table 5, the group that indicates the relative importance of the net heat transferred to the system, $\Xi_{\dot{p},\dot{q}_{net}}$ is still the most influential in the pressurization of both facilities. The mass conservation equation yields the relative importance of the contribution to the total mass of the system by the balance of the mass flow rates, whose value is one. Regarding the groups obtained from the momentum balance, $\Xi_{L/A}$ and Ξ_F have the same values as in the first stage for being only dependent on the geometry of the facilities. Similarly, the contribution to natural circulation phenomena of these groups is substantially lower than that of the natural circulation driving term, since their importance are less than 1/10 of that of Ξ_{Ri}.

The distortion ratios in Table 5 are like those calculated for the first stage. The slight increase in the most important groups ($\Xi_{\dot{p},\dot{q}_{net}}$ and Ξ_{Ri}) is worthy of mention. The distortion of the net heat transfer (ratio equal to 1.18) is attributed to considering constant heat losses when scaling the core power curve, and this distortion increases as the transient progresses. The increase in the distortion of the natural circulation driving term, Ξ_{Ri}, partially justifies the differences in the NC mass flow between the facilities and the distortion of the chronology of events. Despite this, the distortion is not significant (0.67) and the phenomena that take place during the stage are considered well-scaled. This suggests the need for further analyzes to justify the differences in natural circulation, specifically the influence of technological features of ATLAS and LSTF.

Table 5: Summary of the scaling approach results for the NC second stage.

Dimensionless groups	ATLAS groups	ATLAS importance	LSTF groups	LSTF importance	Distortion ratio
$\Xi_{\dot{M},\dot{m}} = \frac{\dot{m}_0}{M_0}\tau_0$	1.00	1.00	1.00	1.00	1.00
$\Xi_{\dot{p},\dot{m}(h_{out}-\mu_m)} = \frac{\tau_0}{\Delta p_0}\frac{\left(\frac{\delta p}{\delta \mu_m}\right)_{v_m,0}}{M_0}\dot{m}_0\left(h_{out,0}-\mu_{m,0}\right)$	-0.30	0.05	-0.40	0.089	0.74
$\Xi_{\dot{p},\dot{q}_{net}} = \frac{\tau_0}{\Delta P_0}\frac{\left(\frac{\delta p}{\delta \mu_m}\right)_{v_m,0}}{M_0}\dot{q}_0$	-5.50	1.00	-4.5	1.00	1.21
$\Xi_{\dot{p},\dot{m}v_m} = \frac{\tau_0}{\Delta P_0}\frac{\left(\frac{\delta p}{\delta v_m}\right)_{\mu_m,0}}{M_0\rho_{m,0}}\dot{m}_0$	2.70	0.50	2.99	0.66	0.90
$\Xi_{L/A} = \frac{\sum(L/A)_i}{(L/A)_0}$	28.1	0.007	23.1	0.004	1.22
$\Xi_{Ri} = \frac{g\overline{\rho_0}\Delta H}{\rho_0 u_0^2}$	4000	1.00	5970	1.00	0.67
$\Xi_F = \sum\left\{\left(\frac{f_i L_i}{2D_{h,i}}+\frac{k_i}{2}\right)\left(\frac{A_0}{A_i}\right)^2\right\}_0$	24.1	0.006	16.30	0.003	1.48

In view of the simulation results, there is a great distortion in the chronology that is not justified by the dimensionless groups. This is because the transfer rate of the properties evaluated for the period of each NC phase roughly preserves the scaling. As natural circulation mass flow is driven by the net power, a more comprehensive analysis of the group on the heat transfer rate, $\Xi_{\dot{p},\dot{q}_{net}}$, may be conclusive. Considering each parameter individually, the existence of significant distortion of the net power and timing is verified, despite their values are compensated and result in a similar dimensionless group in ATLAS and LSTF. On the other hand, technological differences related to steam generators also influence the evolution of the transient. The coolant capacity of ATLAS steam generators is 0.65 m^3 and that in LSTF is 2.7 m^3, each one. Thus, the amount of coolant required to scale the ATLAS experiment according to the scaling ratio of 0.2, does not fit the LSTF steam generators, advancing drying and subsequent events. The temporal distortion will appear in the counterpart transients that involve the complete emptying of the steam generators between these facilities.

The distorting effects of these two aspects have been studied using hybrid models, which can reproduce hypothetical thermohydraulic behaviors. Three models of the LSTF facility that characterize the scaled inventory of the secondary system and the heat losses of ATLAS have been built to reproduce the same SBO scenario. Then, the transients are compared to the ATLAS experiment to verify the test scalability and distortion under new conditions.

For the first analysis, the model denoted as LSTF_Power alters the net power during the test. The core power has been defined from the experimental power supplied in ATLAS and the decay curve results slightly increased. Moreover, the heat transfer coefficients on the pipe walls model have been increased to produce equivalent heat losses to those scaled in ATLAS. These changes lead to the rise

in mass flow along the loops and, at the same time, the extension of the two NC stages up to 5500 s and 8770 seconds, respectively.

The steam generators of the second model, called LSTF_SG, are higher compared to the real ones. Therefore, it is possible to establish the inventory of 3.25 m^3 according to the volume scaling ratio as the initial condition of the test. With this model, compared to the one presented in the previous section, the emptying time of the steam generators is notably extended. Once emptied and when the POSRV opens, the mass flow in the primary system is maintained longer because the core power has decayed.

The third analysis combines both modifications in the model denoted as LSTF_Power+SG. Thus, the largest discrepancies observed between the ATLAS test and the proposed one for LSTF are reduced. Table 6 compares the average net power ratios during each stage ($q_{R,I}$, $q_{R,II}$) and the ratios of their duration ($\tau_{R,I}$, $\tau_{R,II}$) in an ideally scaled scenario, those estimated from the previous simulation with the model called LSTF_Base, and those calculated from the hybrid models. As can be seen, both modifications increase the duration of the natural circulation phase in LSTF, the time ratios reduce, and the combination of improvements in LSTF_Power+SG provides time ratios close to 0.68, expected with ideal scaling.

Regarding the power ratios with the LSTF_Base model, these were not much lower than 0.29, but the need to accurately reproduce the net power supplied to the system has been proven due to the importance of this parameter in the evolution of the transient. This study indicates that counterpart experiments simulating long-term transients will be quite distorted in time at different-scale test facilities. In this SBO scenario, the distortion is caused by the decisive effect of the heat losses in ATLAS. Therefore, different strategies must be implemented to reduce this distortion in the design of the counterpart test. Heat losses at reduced scales can be compensated with fine insulation or surface heating. In addition, detailed analyzes must be carried out to determine the power curves to be programmed.

Table 6: Comparison of power and time ratios with hybrid models.

TRACE5 Model	$q_{R,I}$	$q_{R,II}$	$\tau_{R,I}$	$\tau_{R,II}$
Ideal scaling	0.29	0.29	0.68	0.68
LSTF_Base	0.23	0.25	1.35	1.38
LSTF_Power	0.22	0.28	1.06	1.09
LSTF_SG	0.29	0.26	0.93	1.01
LSTF_Power+SG	0.29	0.30	0.72	0.73

Figure 10 and Figure 11 show the mass flow rate in the loop with pressurizer and the PCT using the LSTF_Power+SG model. It can be seen as in LSTF, despite presenting a scaled mass flow lower than that of ATLAS, it is maintained approximately for the same time. Once natural circulation interrupts, the excursion of the core temperature takes place in advance, which may be due to the technological differences of the vessel and the inventory distribution.

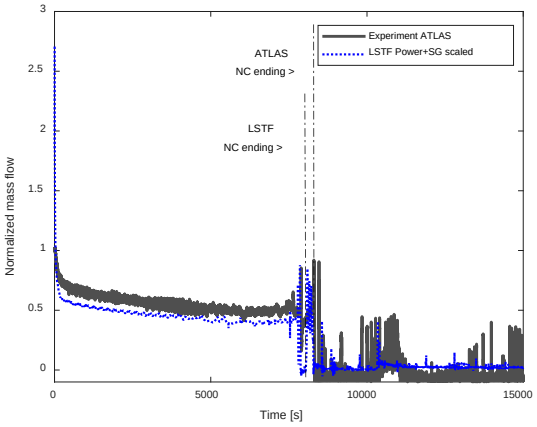

Figure 10: Mass flow rate using a hybrid model.

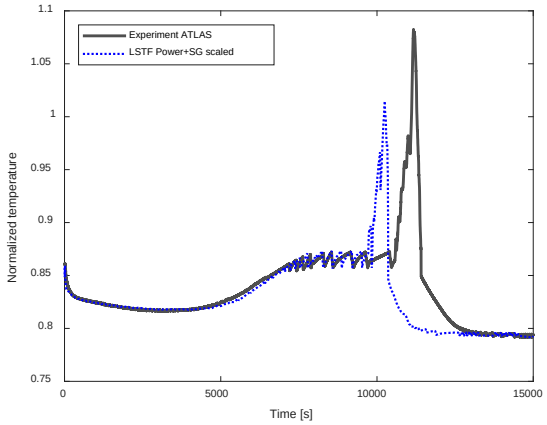

Figure 11: Peak cladding temperature using a hybrid model.

Finally, the dimensionless groups that characterize thermal-hydraulic phenomenology have been recalculated. The LSTF_Power+SG model reduces the distortion referred to the net power of the system, being the distortion ratios for the group $\Xi_{\dot{p},\dot{q}_{net}}$ equal to 0.96 and 1.14 in each stage. The ratios between the dimensionless groups related to the natural circulation driving term (Ξ_{Ri}) are 0.73 and 0.75, and consequently, this distortion is also reduced, since the similarity between the mass flows in ATLAS and LSTF enhances.

5 CONCLUSIONS

The scaling issue has been addressed for several decades; however, it remains a relevant concern in the nuclear safety field since the correct prediction of the behavior of nuclear power plants from experimental databases obtained in scaled test facilities cannot be guaranteed. In this framework, the current work aims to analyze the scaling of an accidental SBO-type scenario between the different-scale test facilities ATLAS and LSTF. The experiment in question is based on the Test A1.1 belonging to OECD-ATLAS project. Starting from the initial and boundary conditions of the experiment, a novel

counterpart test for LSTF is designed, which is simulated using the TRACE5 thermohydraulic code. Continuedly, a dimensionless analysis is applied to the simulation results to verify the scaling methodology for designing counterpart experiments between these facilities and confirm the similarity of results. Then supportive models are used to justify the distortion in the thermohydraulic phenomena. Major results of the work are summarized as follows:

1. The test A1.1 has been studied and its initial and boundary conditions have been scaled applying Ishii's scaling laws for two-phase flow and the geometric ratios between ATLAS and LSTF. Then, both experiments have been simulated with two verified TRACE5 models of the facilities.

2. ATLAS model reproduces accurately the thermal-hydraulic behaviors as far as pressures, temperatures and natural circulation mass flows. Regarding LSTF, the most important phenomena, like the pressurization, the end of the natural circulation and the excursion of the PCT are reproduced in a very similar way but early. This discloses the possibility to predict the sequence of the major events in one of these facilities from the thermal-hydraulic variables in the other one, in this type of accident.

3. The delayed and asymmetric cooling through the auxiliary feedwater system has been proved to be an effective accident management measure at different scales.

4. A scaling analysis is developed at the primary system level to the natural circulation stages. The dimensionless groups derived from the governing equations are evaluated and compared to detect and justify sources of distortion. Thus, the analysis assesses the scaling methodology and confirms the similarity of phenomenology. It, therefore, follows that two causes motivate significant distortion in the chronology; firstly, the overlapping of effects, since the reduced height of ATLAS and its high heat losses contribute to maintaining the flow in the loops, and secondly, the differences in technology affecting the steam generators, the RPV and the flow paths (configuration of bypass or vessel internals). Consequently, this distortion effect is unavoidable during Test A1.1 and other counterpart transients in which natural circulation is a relevant phenomenon, and a proper chronology will not be reproduced.

5. Hybrid models with TRACE5 code enable characterizing a hypothetical test facility to reproduce thermal-hydraulic behaviors and justify scaling distortion. Thus, the suitability of the ATLAS and LSTF to conduct counterpart SBO-type experiments is verified, as well as their limitations in terms of scaling the chronology.

6. Future work will be aimed at studying the distortion in the scaling of counterpart experiments due to the technology of the ATLAS and LSTF facilities.

Acknowledgment

The authors are grateful to the Management Board of the OECD/ATLAS2 Project for their consent to this publication and thank the Spanish Nuclear Regulatory Body (CSN) for the technical and financial support under the agreement CAMP-España. Moreover, this work has been partially supported by the Spanish Ministerio de Ciencia e Innovación under project ENE2017-89029-P.

REFERENCES

1 Chengcheng Deng, Xueyan Zhang, Ye Yang, Jun Yang, Research on scaling design and applicability evaluation of integral thermal-hydraulic test facilities: A review, Annals of Nuclear Energy, Volume 131, 2019, Pages 273-290, ISSN 0306-4549, https://doi.org/10.1016/j.anucene.2019.03.042.

2 Petruzzi, Alessandro, D'Auria, Francesco, 2011. Thermal-hydraulic system codes in nuclear reactor safety and qualification procedures. Sci. Technol. Nucl. Install. 2008.

3 F. D'Auria, G.M. Galassi, Scaling in nuclear reactor system thermal-hydraulics, Nuclear Engineering and Design, Volume 240, Issue 10, 2010, Pages 3267-3293, ISSN 0029-5493, https://doi.org/10.1016/j.nucengdes.2010.06.010.

4 NEA/CSNI, 1996d, CSNI Integral Test Facility Validation Matrix For The Assessment Of Thermal-Hydraulic Codes For LWR LOCA and Transients, NEA/CSNI/R(96)17, Paris (F)

5 Cherubini, M., Giannotti, W., Dino, A., D'Auria, F. Use of the Natural Circulation Flow Map for Natural Circulation Systems Evaluation. Science and Technology of Nuclear Installations. 2008. 10.1155/2008/479673.

6 D'Auria, F., Galassi, G. M., Ingegneri, M. Evaluation of the Data base from High Power and Low Power Small Break Loca Counterpart Tests Performed in LOBI, SPES, BETHSY, and LSTF Facilities, DCMN Report NT237, 1994

7 A. Annunziato, C. Addabbo, G. Briday, et al., "Small break counterpart tests in the LSTF, BETHSY, LOBI and SPES test facilities," in Proceedings of the 5th International Topical Meeting on Nuclear Reactor Thermal Hydraulics (NURETH-5), Salt Lake City, Utah, USA, September 1992.

8 Belsito, S., D'Auria, F., Ingegneri, M., Chojnacki, E., & Gonzalez, R. (1996). Post test analysis of counterpart tests in LOBI, SPES, BETHSY, LSTF facilities performed with the CATHARE2 code. In Jencic, I. (Ed.). Third Regional Meeting: Nuclear Energy in Central Europe, Proceedings, (p. 562). Slovenia: Nuclear Society of Slovenia.

9 Aksan, N. (2008). International standard problems and small break lossof-coolant accident (SBLOCA). Sci. Technol. Nuclear Install. 2008:814572. doi: 10.1155/2008/814572

10 Reocreux, M. (1992). Proceedings of the CSNI Specialist Meeting on Transient Two-Phase Flow - Current Issues in System Thermal Hydraulics (NEA-CSNI-R--1992-12). Rubinstein, M.C. (Ed.). Nuclear Energy Agency of the OECD (NEA)

11 Takeda, T. and Ohtsu, I. (2017) ROSA/LSTF Test and RELAP5 Analyses on PWR Cold Leg Small-Break LOCA with Accident Management Measure and PKL Counterpart Test. Nuclear Engineering and Technology, 49, 928-940. https://doi.org/10.1016/j.net.2017.03.004

12 Belaid, S., Freixa, J., Zerkak, O., 2010. Analysis of the Test OECD-PKL2 G7.1 with the Thermal-Hydraulic System Code TRACE. U.S. Nuclear Regulatory Commission, Washington, DC, NUREG/IA-0432.

13 Carlos, S., et al., 2016. Post-test analysis of the ROSA/LSTF and PKL counterpart test. Nucl. Eng. Des. 297, 81–94.

14 Takeda, T. (2018) ROSA/LSTF Test and RELAP5 Code Analyses on PWR Hot Leg Small-Break LOCA with Accident Management Measure Based on Core Exit Temperature and PKL Counterpart Test. Annals of Nuclear Energy, 121, 594-606. https://doi.org/10.1016/j.anucene.2018.08.023

15 Yusun Park, Byoung-Uhn Bae, Jong-Rok Kim, Seok Cho, Kyoung-Ho Kang, Ki-Yong Choi, Counterpart test for LSTF 1% cold-leg break LOCA (SB-CL-32) utilizing ATLAS test facility, Nuclear Engineering and Design, Volume 370, 2020, 110912, https://doi.org/10.1016/j.nucengdes.2020.110912.

16 Takeda, T., 2018b. ROSA/LSTF test and RELAP5 code analyses on PWR 1% vessel upper head small-break LOCA with accident management measure based on core exit temperature. Nuclear Engineering and Technology 50 (8), 1412–1420. https://doi.org/10.1016/j.net.2018.08.004.

17 Y. Park. Test Report on the OECD-ATLAS2 B5.1 Test: Counterpart Test for 1% SBLOCA at Reactor Pressure Vessel Top of LSTF with Accident Management Action and Gas Inflow. OECD ATLAS2 TR 20 03. KAERI. 2020.

18 Kyoung-Ho Kang, Byoung-Uhn Bae, Jong-Rok Kim, Yu-Sun Park, Jae-Bong Lee, Seok Cho, Nam-Hyun Choi, Ki-Yong Choi. Integral effect test results on the effect of asymmetric supply of feedwater during a station blackout transient of pressurized water reactor. Annals of Nuclear Energy, Volume 149, 2020, 107837, ISSN 0306-4549, https://doi.org/10.1016/j.anucene.2020.107837.

19 KAERI, 2014. Scaling Analysis Report of the ATLAS Facility. Korea Atomic Energy Research Institute, KAERI/TR-5465/2014.

20 The Rosa-V Group, 2003. ROSA-V Large Scale Test Facility (LSTF) System Description for the Third and Fourth Simulated Fuel Assemblies. Japan Atomic Energy Agency (JAEA). Technical Report JAERI-Tech 2003-037.

21 Nakamura, H., et al., 2009. Overview of recent efforts through ROSA/LSTF experiments. Nuclear Engineering and Technology, 41 (6), 753–764.

22 USNRC, 2010. TRACE V5.0 USER'S MANUAL. In: Modeling Guidelines, vol. 2. U.S. Nuclear Regulatory Commission, Washington, DC.

23 Condie, K G, Larson, T K, Davis, C B, and McCreery, G E. Evaluation of integral continuing experimental capability (CEC) concepts for light water reactor research: PWR scaling concepts. United States: N. p., 1987. Web. doi:10.2172/6665765.

24 M. Lorduy-Alós, S. Gallardo, G. Verdú, Simulation studies on natural circulation phenomena during an SBO accident, Applied Thermal Engineering, Volume 139, 2018, Pages 514-523, ISSN 1359-4311, https://doi.org/10.1016/j.applthermaleng.2018.04.130.

25 M. Suzuki, K. Tasaka, M. Shiba. Heat loss and fluid leakage tests of the ROSA-III facility. JAERI M 9834. 1981.

26 Choi, K.Y., Park, H.S., Euh, D.J., Kwon, T.S., Baek, W.P., 2017. Simulation capabilities of the ATLAS facility for major design-basis accidents. Nuclear Technology, 156:3, 256-269.

27 Song, C.-H., 2006. Scaling of the multi-dimensional thermal-hydraulic phenomena in advanced nuclear reactors. Proc. Fifth Korea-Japan Symposium on Nuclear Thermalhydraulics and Safety (NTHAS-5), Nov. 26-29 2006, Jeju, Korea.

28 Ishii, M., Kataoka, I., 1983. Similarity analysis and scaling criteria for LWR's under single-phase and two-phase natural circulation. Argonne National Laboratory, NUREG/CR-3267, ANL-83-32.

29 M. Ishii and N. Zuber, Thermally Induced Flow Instabilities in Two-phase Mixtures," 4th Int. Heat Trans. Conf., Paris, paper B5.11 (1970).

30 M. Ishii and 0.C. Jones, Jr., Derivation and Application of Scaling Criteria for Two-phase Flows, Two-phase Flows and Heat Transfer, Proc.NATO Advanced Study Institute, Istanbul, Turkey, Vol. 1, p.163 (1976).

31 Wulff, W., Rohatgi, U., 1998. System Scaling for the Westinghouse AP600 Pressurized Water Reactor and Related Test Facilities. USNRC Report, Brookhaven National Laboratory, NUREG/CR-5541.

32 Liao, J., 2016. System scaling analysis for modeling small break LOCA using the FULL SPECTRUM LOCA evaluation model. Annals of Nuclear Energy, 87, 443-453.

33 M. Lorduy-Alós, S. Gallardo, G. Verdú, Scaling analysis of an IBLOCA counterpart test between the ATLAS and LSTF facilities, Progress in Nuclear Energy, Volume 127, 2020, 103460, ISSN 0149-1970, https://doi.org/10.1016/j.pnucene.2020.103460.

34 Banerjee, S., Ortiz, M.G., Larson, T.K., Reeder, D.L., 1997. Top-Down Scaling Analyses. Methodology for AP600 Integral Tests, INEL-96/0040, May 1997.

35 Wulff, W., 1996. Scaling of thermohydraulic systems. Nuclear Engineering and Design, 163, 359–395.

36 IAEA, 2005. Natural Circulation in Water Cooled Nuclear Power Plants –Phenomena, Model, and Methodology for System Reliability Assessments. IAEA, Vienna (IAEA-TECDOC-1474).